Direct Observation of Acoustical Activity in α Quartz*

A. S. Pine
Lincoln Laboratory, Massachusetts Institute of Technology, Lexington, Massachusetts
(Received 9 February 1970)

A rotation of the polarization of microwave-frequency (1.05–1.40 GHz) shear waves propagating close to the optical axis in α quartz has been observed. This constitutes the first direct ultrasonic measurement of the phenomenon of acoustical activity predicted by Portigal and Burstein. The magnitude of the acoustical activity is in good agreement with that calculated from a recent Brillouin-scattering determination of the linear wave-vector–velocity splitting of the two transverse-acoustic normal modes. A rotary power of ~3–5 rad/cm is observed at these frequencies; the sense of the rotation is opposite that of the optical activity.

INTRODUCTION

The phenomenon of acoustical activity, predicted by Portigal and Burstein,[1] is the mechanical analog of optical activity. In its simplest form, the plane of polarization of a shear wave rotates as it propagates through a crystal. The first direct ultrasonic observation of this effect is reported here for shear waves propagating close to the c axis in α quartz. The dispersion of the rotary power is measured for phonon frequencies between 1.05 and 1.40 GHz. Also the sense of the acoustical activity is found to be opposite that of the optical activity in the same sample. This is explained here group theoretically.

Portigal and Burstein[1] have shown that acoustical activity is a result of first-order spatial dispersion in the transverse-acoustic (TA) phonon spectrum near the Brillouin-zone center for certain optically active crystals. In particular, the TA phase velocities are split proportionally to the wave vector along the c axis in the uniaxial crystal classes C_3, C_4, C_6, D_3, D_4, and D_6, and along the [100] and [111] axes in the cubic classes T and O. The two transverse modes are right and left circularly polarized so that the phase-velocity difference leads to the progressive rotation of the displacement vector of an incident linearly polarized shear wave.

The linear wave-vector dispersion in the TA phase velocity along the c axis in α quartz and the circular eigenmode polarizations were confirmed recently by Brillouin scattering.[2] Some of the results of that preliminary study are recapitulated here for illustrative purposes though the details are left for the reference. The light scattering experiment probes phonons in the 30-GHz range for which the fractional velocity splitting of the TA doublet is ~1%. This result may be extrapolated to the lower-frequency ultrasonic regime to predict the magnitude of the acoustical activity. The measured rotary power is in good agreement with this prediction when the anisotropy effects due to slightly off-axis propagation are taken into account. Since the observation of acoustical activity is so sensitive to this anisotropy, such effects are discussed here thoroughly.

The lifting of the degeneracy of the shear-wave velocities at finite wave vector in quartz was also exhibited in the neutron scattering results of Elcombe.[3] This splitting is closely related to linear wave-vector shifts in the optical phonon spectrum of quartz as observed by Raman scattering.[4] Pine and Dresselhaus[4] discuss the general symmetry considerations for this effect and relate it to the phenomenon of vibration-induced infrared optical activity.

THEORETICAL CONSIDERATIONS

The magnitude of the acoustical activity may be predicted from the observed splitting of the shear-wave doublet in the Brillouin spectrum. High-resolution Brillouin spectra obtained by backscattering 5017-Å argon-laser light along the c axis in α quartz are presented in Fig. 1. The upper interferometer trace, showing the Stokes and anti-Stokes TA doublets, is taken with linearly polarized laser light; the lower traces with circular polarization. These selection rules demonstrate that the TA modes are oppositely circularly polarized. The mean phonon frequency is $2n\bar{v}/\lambda = 28.9$ GHz, where n is the ordinary index of refraction at wavelength λ and $\bar{v} = \frac{1}{2}(v_f + v_s) = (c_{44}/\rho_0)^{1/2}$ is the average phase velocity of the fast and slow waves in terms of the usual elastic constant and density. The free spectral range of the interferometer is 1.5 GHz so the doublet splitting is 276 MHz.

Since the splitting is proportional to the wave-vector q or the frequency ν, the difference in the phase velocities of the fast and slow waves propagating exactly along the c axis is

$$(v_f - v_s)/\bar{v} = \gamma \nu \,. \tag{1}$$

For α quartz, $\gamma = 3.3 \times 10^{-4}$/GHz as determined from the Brillouin data. A rough quantitative measure of γ could also be obtained from Elcombe's

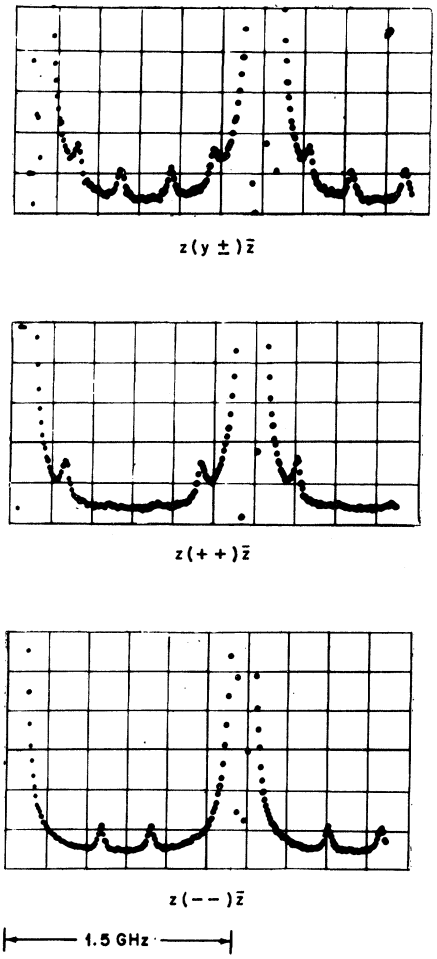

FIG. 1. Brillouin-scattering spectra from shear-wave doublet in α quartz. Backscattering along c axis with $\lambda = 5017$ Å. Upper trace: incident polarization linear. Middle trace: incident polarization right circular. Lower trace: incident polarization left circular.

neutron scattering data. This rather small velocity splitting for a wave vector along the c axis results in a substantial polarization rotation

$$\rho = \pi\nu l(v_s^{-1} - v_f^{-1}) \simeq \pi\gamma\nu^2 l/\bar{v} \qquad (2)$$

of $\sim 127°$ at 1 GHz for a crystal length $l = 1$ cm. Frequencies in this range are convenient experimentally since the ultrasonic attenuation lengths are several cm at room temperature.

When the phonon wave vector is offset from the trigonal c axis by an angle θ, the velocity splitting increases rapidly, due to normal acoustical birefringence, and the eigenmodes become elliptically polarized. These effects are illustrated for α quartz in Fig. 2 where the velocity surfaces near the c axis are plotted for frequencies of 28.9 GHz and 0 Hz. The higher-frequency curves correspond to the Brillouin data; the zero-frequency curves represent the ordinary and extraordinary waves computed from the well-known elastic constants.

In the acoustical-activity experiment, standard microwave ultrasonic techniques are used to piezoelectrically generate a linearly polarized shear wave in a reentrant (polarizer) cavity at a surface well-oriented normal to the c axis of an α-quartz sample. The polarization state of the shear wave transmitted to a parallel surface is detected in another similar (analyzer) cavity. Imperfect orientation of the sample affects the measured rotation when the birefringence splitting due to off-axis propagation is comparable to the on-axis splitting. At 1 GHz in α quartz this occurs for $\theta \sim 2'$, which is close to the experimental capability for orienting the crystal. Under such circumstances, the acoustical activity may be sorted out from the birefringence using the classical theories for the analogous problem in crystal optics.

The velocity surfaces and polarization ellipticity for the coupled TA modes may be calculated from the dynamical equations-of-motion matrix given by Portigal and Burstein.[1] For a small offset angle $\theta \ll 1$ rad, the two phase-velocity surfaces obtained from the secular equation are

$$v_{f,s}^2 = (c_{44}/\rho_0)\{1 \pm [(2\theta c_{14}/c_{44})^2 + (\gamma\nu)^2]^{1/2}\}, \qquad (3)$$

and the ellipticity (minor-to-major axis ratio) of the normal modes is

$$\epsilon = \frac{\gamma\nu}{(2\theta c_{14}/c_{44}) + [(2\theta c_{14}/c_{44})^2 + (\gamma\nu)^2]^{1/2}} . \qquad (4)$$

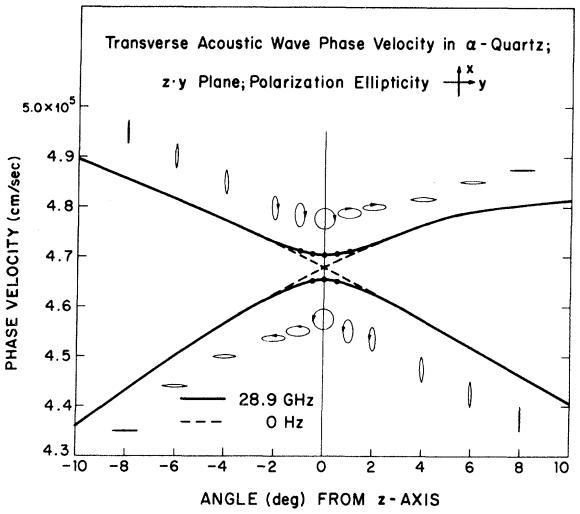

FIG. 2. Shear-wave velocity surfaces and polarizations near c axis in α quartz illustrating acoustical anisotropy.

The orthogonal major axes of the two ellipses are along $\frac{1}{2}\phi \pm \frac{1}{4}\pi$, where ϕ is the azimuth of the wave vector relative to the crystal x axis. An incident shear wave linearly polarized at an angle α from the major axis of the fast normal mode is decomposed into the two elliptical waves. After traveling through a crystal of length l, the fast wave is advanced in phase by

$$\Delta = 2\pi\nu l(v_s^{-1} - v_f^{-1}) \simeq (2\pi\nu l/\bar{v})[(2\theta c_{14}/c_{44})^2 + (\gamma\nu)^2]^{1/2} . \quad (5)$$

The ellipticity ϵ and relative phase Δ have precisely the same form as the analogous problem of light propagation in an optically active birefringent crystal.[5] Therefore, the state of polarization of the recombined wave at l is obtained using the mathematical techniques developed for crystal optics. The simplest of these is the graphical Poincaré sphere method discussed in detail by Ramachandran and Ramaseshan.[6] Such analyses are based on infinite plane-wave theory, so the diffraction and refraction effects of a finite geometry must be considered separately.

Refraction occurs when the phase-velocity surfaces are not spherical, as in Eq. (3). Here the acoustical energy propagation does not coincide with the wave vector. In the absence of acoustical activity, Waterman[7] has shown that this leads to the phenomenon of conical refraction about a trigonal axis where the group velocity deviates from the wave vector by an angle $\psi = \tan^{-1}(c_{14}/c_{44})$ ($\simeq 17^\circ$ for α quartz). Merkulov and Yakovlev[8] demonstrated this refraction in α quartz by a shadow display of c-axis shear waves at such a low frequency (25 MHz) that acoustical activity is unimportant. However, at higher frequencies the distortion in the phase-velocity surfaces caused by the acoustical activity results in a deviation of the group and phase velocities that ranges from zero to a maximum of $\sim\psi$ as the wave vector is slightly offset by angle θ from the c axis. A small angular spread of wave vectors due to diffraction results, therefore, in a much larger spread in beam directions.

EXPERIMENTAL CONSIDERATIONS

In this experiment the sample is prepared to minimize the effects of linear birefringence and conical refraction. The surface normals, which define the direction of the phonon wave vector to within diffraction limits, were oriented to within $2'$ of the crystal c axis. This orientation is accomplished optically using the interference pattern of the uniaxial crystal through crossed polarizers.[9] These surfaces were polished flat to $\frac{1}{10}$ of the wavelength of red light and parallel to within $5''$. The diameter of the rod is chosen such that $d/l < \tan\psi$. Thus any beam refracted at angle ψ strikes the rough-ground sides and is not detected. Because of the significant diffraction-angle spread $\delta\theta \sim \bar{v}/\nu d$, the diameter is not made arbitrarily small. The sample dimensions are $l = 1.85$ cm and $d = 0.53$ cm so that $\delta\theta \sim 3'$; this exceeds the misorientation and causes much of the beam to be lost on refraction. ZnO film transducers, less than 1 μ thick, were sputtered onto the ends of the quartz rod with the ZnO c axis normal to the surfaces. As seen from the piezoelectric tensor[5] for C_{6v} symmetry, fields parallel to the surface couple to shear waves polarized in the same directions, and fields normal to the surface generate longitudinal waves.[10]

The reentrant-microwave polarizer and analyzer cavities are shown schematically in Fig. 3(a). The cavities are tunable from 1.0 to 1.5 GHz by means of plate T. The quartz rod Q is located in an eccentric Teflon mount E to one side of a wedged post. The rf fields are normal to the wedge facets, so they produce both a longitudinal-acoustic wave and a shear wave uniformly polarized normal to the dihedral. The same configuration is used in the analyzer cavity which may rotate around the crystal. The polarizer-analyzer extinction ratio is better than 100:1 as tested by observing the orientation dependence of the two shear modes in an x-cut quartz rod.

Traces of the reflected and transmitted ultrasonic pulses in the z-cut sample are given in Figs. 3(b), 3(c), and 3(d) with the transit times noted. The echo [Fig. 3(b)] provides information about tuning and attenuation, but not about the rotary power. Reciprocity requires that the effects of acoustical activity are reversed upon reflection. The transmitted pulses, with the analyzer oriented for maximum shear-wave detection, are shown in Fig. 3(c), and for minimum in Fig. 3(d). The longitudinal fields are not affected by the position of the analyzer indicating that the cavity is not detuned by its rotation. The net rotation of the major polarization axis of the transmitted shear wave in Fig. 3(c) is $-45^\circ \pm n \times 180^\circ$ at 1.2 GHz. The correct sign and integer n for the rotary power is determined by varying ν and comparing with theory.

RESULTS

The dispersion of the rotation is plotted in Fig. 4. The theory of Eq. (2), for propagation exactly along the c axis, is shown as the solid line. The dotted lines are the results of a Poincaré-sphere graphical analysis for a wave vector off-axis by $1.5'$. Since the misorientation is immeasurably small by independent optical means, the azimuth

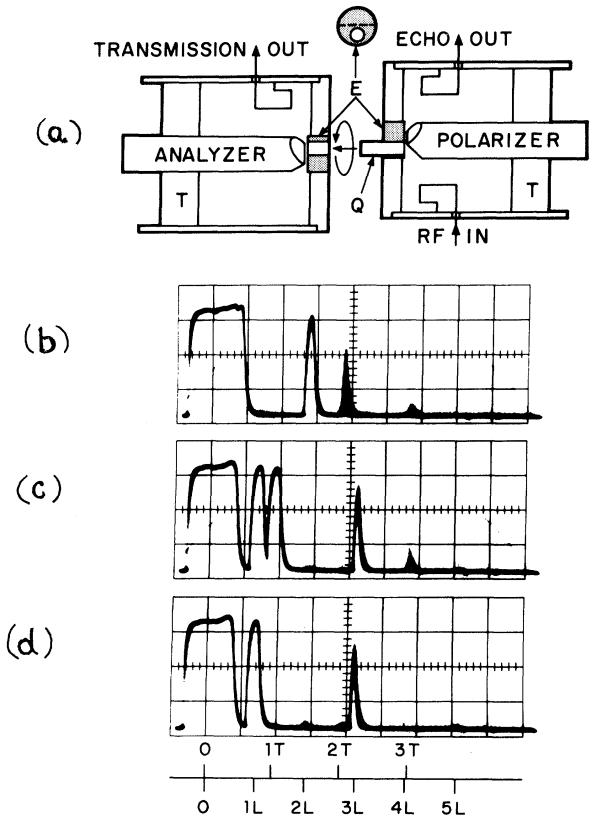

FIG. 3. Shear-wave generation and detection scheme for acoustical activity measurement. (a) Microwave polarizer and analyzer cavities; analyzer fits over, and rotates around, the quartz crystal Q. T is a sliding tuning plate; E is an eccentric Teflon mount. (b) Ultrasonic echoes at 1.2 GHz. (c) Ultrasonic transmission; analyzer rotated (−45°) for maximum shear-wave signal. (d) Ultrasonic transmission; analyzer rotated (+45°) for minimum shear-wave signal. Transit times for c-axis transverse and longitudinal waves indicated below; time scale 2 μsec/cm for crystal length 1.85 cm.

ϕ is unknown. Therefore, the incident polarization angle α cannot be determined, and the extreme cases of $\alpha = 0°$ and 45° have been plotted. The data shown are for constant α. The drastic theoretical fluctuations in ρ below 1 GHz for $\theta = 1.5'$ represent the dominance of the linear birefringence over the acoustical activity. Even at frequencies high enough for acoustical activity to dominate, the increased phase shift due to the birefringence contributes substantially to the rotation. Agreement of the data with the Poincaré-sphere theory is remarkable considering the sizable angular spreads due to diffraction and refraction. Fortunately the angular spread in the phase fronts, coherently detectable over the whole surface, is smaller than the diffraction spread by a factor of ~ 2. These complications, however, probably account for an observed rotation variation (~ +10° to − 30° at any given frequency) on change of α, which is larger than expected from the Poincaré theory.

The sense of the acoustical rotary power is measured to be opposite the optical activity in the same sample. The sign of the acoustical activity can be inferred from space-group character and compatibility tables[11] and the neutron scattering phonon-dispersion data[3] as demonstrated in the Appendix. In quartz these considerations predict a rotation of the plane of polarization of the shear wave opposite to the sense of the crystal screw axis. This is consistent with a previous structural determination of α quartz showing the screw axis and the optical activity to have the same sense.[12] Interestingly, the theoretical phonon-dispersion curves in trigonal Se[13] or Te[1,14] (isomorphous to α quartz) indicate that the TA phonon branches along the c axis are inverted from those of quartz. Therefore, in these materials, the acoustical activity would follow the screw axes.

Acoustical activity in crystals of C_6 or D_6 symmetry should be observable with a negligible contribution from acoustical birefringence. Since c_{14}

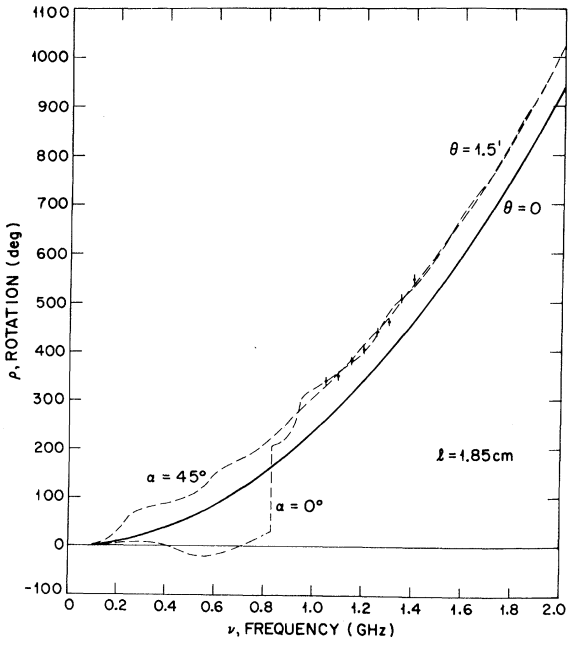

FIG. 4. Acoustical activity in α quartz. Rotation of shear-wave polarization in sample of length 1.85 cm. Solid curve for wave vector exactly along c axis. Dashed curves for wave vector at $\theta = 1.5'$ from c axis; incident polarization angle α from fast transverse-mode major axis.

is zero in these crystals, the velocity splitting about the c axis due to birefringence is only second order in θ, and the conical refraction is eliminated. A prime candidate for measurement, were it not for the high temperatures involved, would be hexagonal β quartz which should have approximately the same acoustical activity as α quartz.

Note added in proof. (a) Recent neutron scattering measurements in Te by B. M. Powell and P. Martel [Bull. Am. Phys. Soc. 15, 810 (1970)] indicate the same TA ordering along the Δ axis as in α quartz, though the magnitude of the splitting is considerably smaller. Thus the sense of the acoustical activity in Te would be opposite the screw axis. (b) Acoustical activity in α quartz has been observed subsequently at higher frequencies ~9 GHz and lower temperatures ~4 °K by J. Joffrin and A. Levelut. Their rotary power, assuming no temperature dependence and scaling by ν^2, is ~17% below that reported here – a discrepancy which is within their stated experimental accuracy. Presumably their work will appear in the French literature shortly.

ACKNOWLEDGMENTS

The author is grateful to Dr. G. Dresselhaus for many essential discussions – in particular for the group-theoretical arguments giving the sign of the rotary power. Much appreciation is due Professor E. Burstein for stimulating the author's interest in this phenomenon. Special thanks go to C. D. Wyche for preparing the sample and building the cavities and to Dr. H. I. Smith for providing the the ZnO transducers.

APPENDIX: SENSE OF THE ACOUSTICAL ACTIVITY

The sense of the acoustical rotary power relative to the crystal screw axis can be determined group theoretically if the phonon-dispersion relations are known along this axis. This dispersion has been obtained by neutron scattering in α quartz.[3] The necessary group theory is contained in the character table for a general point along the screw axis of the Brillouin zone. An example for space-group symmetry $D_3^4(P3_1\,21)$ is given in Table I.[11] In this table $\omega = e^{i2\pi/3}$, $\tau = e^{iqc/3}$, c is the unit-cell dimension along the trigonal axis, T is a translation of $\frac{1}{3}c$ in the positive z direction, and C_3 is a *positive* 120° rotation about z with the characteristics

TABLE I. Δ-axis character.

	E	C_3T	$(C_3T)^2$
Δ_1	1	τ	τ^2
Δ_2	1	$\omega\tau$	$\omega^2\tau^2$
Δ_3	1	$\omega^2\tau$	$\omega\tau^2$

$$\{C_3\}\begin{bmatrix} x \\ y \\ z \\ x+iy \\ x-iy \end{bmatrix} = \begin{bmatrix} -\frac{1}{2}(x-\sqrt{3}\,y) \\ -\frac{1}{2}(\sqrt{3}\,x+y) \\ z \\ \omega^2(x+iy) \\ \omega(x-iy) \end{bmatrix} . \tag{A1}$$

The compatibility relations[11] for the Γ point ($q=0$) are $\Delta_1 \to \Gamma_1$ or Γ_2 and $\Delta_2+\Delta_3 \to \Gamma_3$; and for the A point ($q=\pi/c$), $\Delta_2 \to A_1$ or A_2 and $\Delta_1+\Delta_3 \to A_3$.

The eigenvectors of the two TA modes must be related to the irreducible representations along the Δ axis. If the two waves have velocities $v_\pm$, frequency ν, and propagate in the positive z direction, then

$$\begin{aligned} u^\pm(z,t) &\equiv \mathrm{Re}[(u_x \pm iu_y)\,e^{i(qz-2\pi\nu t)}] \\ &= u_x \cos 2\pi\nu(t-z/v_\pm) \\ &\quad \pm u_y \sin 2\pi\nu(t-z/v_\pm) . \end{aligned} \tag{A2}$$

Since the modes are circularly polarized, we have $|u_x| = |u_y|$. The upper (+) sign refers to a temporal rotation in the same sense (positive) as the C_3 operation defined previously. Operations on an eigenvector are inverse to those on the coordinates, so $\{C_3T\}u^+ = \omega\tau u^+$ and $\{C_3T\}u^- = \omega^2\tau u^-$. Thus u^+ may be identified with Δ_2, and u^- with Δ_3.

The rotation ρ, obtained by recombining the two circular modes at $z=l$ if a linearly x-polarized shear wave is launched at $z=0$, is

$$\rho \equiv \tan^{-1}[(u_y^+ + u_y^-)/(u_x^+ + u_x^-)] = \pi\nu l(v_-^{-1} - v_+^{-1}) . \tag{A3}$$

Therefore ρ is a positive rotation if $v_+ > v_-$, and negative if $v_+ < v_-$. This is the well-known result that the rotation is in the same sense as the fast circular mode.

In α quartz the slow wave is compatible with a singlet at the A point,[3] so for D_3^4 symmetry $v_+ < v_-$ (since $u^+ \to \Delta_2$), and the acoustical rotary power is opposite the sense of the crystal screw axis. For the enantiomorphic space group $D_3^6(P3_221)$, the character table is the same except that T is a translation of $\frac{2}{3}c$ and $\tau = e^{i2qc/3}$. In this case the A-point compatibility relations are $\Delta_3 \to A_1$ or A_2 and $\Delta_1+\Delta_2 \to A_3$. Thus u^-, which goes as Δ_3, is the slow-wave singlet, and the relative sense of the acoustical activity and the screw axis is preserved. Lattice-dynamical-model calculations for Se[13] and Te[14] indicate that the TA mode connected with the A-point singlet is the fast mode. This implies that the acoustical activity follows the sense of the screw axis in Se and Te.

*Work supported by the Department of the Air Force.

[1]D. L. Portigal and E. Burstein, Phys. Rev. 170, 673 (1968).

[2]A. S. Pine, J. Acoust. Soc. Am. (to be published).

[3]M. M. Elcombe, Proc. Phys. Soc. (London) 91, 947 (1967).

[4]A. S. Pine and G. Dresselhaus, Phys. Rev. 188, 1489 (1969).

[5]J. F. Nye, *Physical Properties of Crystals* (Oxford U. P., London, 1964), Chap. XIV.

[6]G. N. Ramachandran and S. Ramaseshan, in *Handbuch der Physik*, edited by S. Flugge (Springer-Verlag, Berlin, 1961), Chap. XXV, p. 1.

[7]P. C. Waterman, Phys. Rev. 113, 1240 (1959).

[8]L. G. Merkulov and L. A. Yakovlev, Akust. Zh. 8, 99 (1962) [Soviet Phys. Acoust. 8, 72 (1962)].

[9]J. P. Mathieu, in *Handbuch der Physik*, edited by S. Flugge, (Springer-Verlag, Berlin, 1957), Chap. XXVIII, p. 407.

[10]Actually with higher-sensitivity microwave detection apparatus, the experiment could be performed without ZnO transducers since the z-cut quartz is weakly piezoactive for shear waves (polarization perpendicular to the electric field). Transmitted signals are barely observable here with only one end ZnO coated, though the data shown are taken with both ends coated.

[11]S. C. Miller and W. F. Love, *Tables of Irreducible Representations of Space Groups* (Pruett Press, Boulder, Colo., 1967.

[12]A. DeVries, Nature 181, 1193 (1958).

[13]R. Geick, U. Schröder, and J. Stuke, Phys. Status Solidi 24, 99 (1967).

[14]M. Hulin, J. Phys. Chem. Solids Suppl. 21, 135 (1965).

PHYSICAL REVIEW B VOLUME 2, NUMBER 6 15 SEPTEMBER 1970

Calculation of the Band Structure and Optical Constants of Diamond Using the Nonlocal-Pseudopotential Method

Louis A. Hemstreet, Jr.

Department of Physics, University of California, Davis, California 95616

and

C. Y. Fong*

Inorganic Materials Research Division, Lawrence Radiation Laboratory, University of California, Berkeley, California 94720

and

Department of Physics, University of California, Davis, California 95616

and

Marvin L. Cohen†‡

Department of Physics and Inorganic Materials Research Division, Lawrence Radiation Laboratory, University of California, Berkeley, California 94720

(Received 9 March 1970)

The electronic band structure and optical constants of diamond are calculated using the empirical-pseudopotential method with an additional $\ell=1$ nonlocal term $V_{NL}(\vec{r})$ added to account for the strong potential experienced by p electrons in the core region. $V_{NL}(\vec{r})$ strongly affects the p-like conduction bands, and the resulting band structure yields a plot of $\epsilon_2(\omega)$, the imaginary part of the dielectric function, which is in satisfactory agreement with experiment. In addition, the temperature-dependent peak at 7.8 eV in the optical spectrum, whose origin has been somewhat of a mystery, is identified with optical transitions beginning at L and extending out along the Λ direction in the Brillouin zone.

INTRODUCTION

The band structure of diamond has been extensively studied by several authors[1-5] in recent years. We will focus here on those calculations utilizing the empirical-pseudopotential method[1-3] (EPM) with the aim of extending these calculations. Since good pseudopotential calculations for silicon are presently available in the literature,[6] it would seem to be possible to combine the best sets of form factors for C and Si to determine a consistent band structure for SiC. Furthermore, the form factors for C can be used to determine the symmetric part of the form factors for BN and BP. However, before proceeding directly toward these goals, further improvement on the presently available diamond calculations is considered necessary as the resulting band structures do not yield a totally satisfactory fit to the experimental optical data. In particular, the calculated ϵ_2 spectra of